Journal of Soils and Sediments (2018) 18:2935–2947
https://doi.org/10.1007/s11368-018-1980-9

SOILS, SEC 3 • REMEDIATION AND MANAGEMENT OF CONTAMINATED OR DEGRADED LANDS • RESEARCH ARTICLE

The transformation and migration of selenium in soil under different Eh conditions

Jianxin Fan[1,2] · Yu Zeng[1] · Jiaoxia Sun[1]

Received: 8 January 2018 / Accepted: 20 March 2018 / Published online: 27 March 2018

Abstract

Purpose Soil selenium (Se) sequestration and transformation, which are strongly controlled by soil redox conditions, are critical for understanding the mobility and bioavailability in the environment. Thus, the effect of redox potential on Se transformation was investigated for exploring the release mechanism of Se in soil.

Materials and methods Soils were incubated under anoxic condition in four treatments at room temperature over 56 days, and the soil solution pH, Eh, and Fe and Se concentrations were measured at given reaction time. The sequential extraction and X-ray photoelectron spectroscopy (XPS) were used to obtain the species distribution of Se in soil. High-resolution transmission electron microscopy (HR-TEM) was employed to observe morphology characteristic of soil.

Results and discussion Parts of soil Se can be released into solution, and Se speciation in soil changed during the incubation period. XPS and sequential extraction analyses revealed that the primary speciation of Se in soil was elemental Se, and metallic selenides were formed under aerobic condition. Moreover, XPS and HR-TEM data revealed the crystalline state of iron oxides in soil changed after anoxic incubation, and certain amorphous iron oxides were formed.

Conclusions Se release is activated by short-term incubation, whereas Se can be transformed into less soluble state after long-term incubation. Organic matter takes extremely an important role in Fe oxide reductive dissolution and Se transformation. This study is useful to understand the environmental behaviors of Se and enhance the application of Se fertilizers effectively and safely in Se deficiency area.

Keywords Iron oxides · Redox potential · Selenium · Soil

1 Introduction

Selenium is an essential micronutrient element for human and animal growth (Rotruck et al. 1973), and it affects human health with a dietary intake outside the range of 40 μg per day (Combs 2007) to 400 μg per day (Medicine 2000). Selenium levels in human body are controlled through diet, and selenium levels in food generally depend on content and form in soil (Sathe et al. 1992). However, large areas of soils contain low selenium content. In China, the extensive Se-poor belt is located in the eastern farming region and accounts for 72% of arable land soil with extremely low selenium levels (< 0.05 mg kg^{-1}) (Tan et al. 2002). Because dietary Se intake is the most practical approach for Se nutrition, biofortification of Se in agriculture through selenium-enriched fertilizers has been proposed to elevate the selenium concentration in plants, improve the selenium content in human body, and effectively decrease the Kashin-Beck disease (KBD) in numerous areas (Winkel et al. 2015).

Nevertheless, low selenium bioavailability in soil may be responsible for selenium deficiency in human (Rayman 2008), and the reduction of exogenous selenate and selenite in soil

Responsible editor: Kitae Baek

Electronic supplementary material The online version of this article (https://doi.org/10.1007/s11368-018-1980-9) contains supplementary material, which is available to authorized users.

✉ Jianxin Fan
jxfanw@cqjtu.edu.cn

[1] Chongqing Engineering Laboratory of Environmental Hydraulic Engineering, Chongqing Municipal Development and Reform Commission, Chongqing Jiaotong University, Chongqing 400074, China

[2] College of Resources and Environment, Southwest University, Chongqing 400715, China

can diminish selenium bioavailability. Therefore, the migration and transformation of selenium into soil, soil minerals, soil organic matter (SOM), and clay should be investigated to understand the biogeochemical characteristics of selenium. Numerous studies analyzed the sorption behaviors of selenium in soils and soil minerals. For instance, Hingston et al. studied the effect of pH and negative charge on selenite sorption by goethite in 1968 (Hingston et al. 1968). Moreover, the exchange constant for OH^- and SeO_3^{2-} was calculated in 1990 (Zhang and Sparks 1990), revealing the selenate fixed on goethite through electrostatic adsorption and selenite absorbed onto goethite by ion exchange. Manceau and Charlet (1994) showed that selenate forms inner-sphere surface complexes on goethite and hydrous ferric oxide, such as phosphate and selenite, and binuclear bridging complexes with A-type OH groups. Scholars also found that adsorption mechanisms are strongly affected by both pH and ionic strength. Soil is a complex material containing hydro-oxide minerals, silicon oxide, humus, clays, and biotic compartments. Soil properties and environmental factors can influence sorption characteristics. Dhillon and Dhillon (1999) reported that soil pH affects selenium sorption onto soils and that acidic soils show higher affinity for selenium than basic soils, because that SO_3^{2-} species were preferential adsorbed on highly positive surface sites, with the anion displacing more than one OH^- from surface and forming binuclear surface complexes, and HSO_3^- species increased and adsorbed with displacing one OH^- in acid soil. Lessa et al. (2016) investigated selenium (VI) adsorption onto different soils and noted that clayed soils exhibit higher sorption capacity in clayed soils than sandy soils.

However, the redox reaction is an important process in soil, which can change the speciation and bioavailability of selenium. Previous studies on the redox behavior of selenium focused on the reaction on soil minerals and SOM, which have strong affinity with Se and other nutriments or contaminants (Masscheleyn and Patrick 1993; Shen et al. 2009; Xu et al. 2011; Fan et al. 2014; Schulz-Zunkel et al. 2015). Myneni et al. (1997) reported that Se(VI) reduced to Se(IV) and Se(0) in the presence of chlorite and that Se(VI) reduction can occur by coprecipitation and adsorption pathways when anoxic conditions are created in Se-contaminated sediments. Chakraborty et al. (2010) determined that Fe(II) can enhance Se(IV) reduction on calcite. The mobility of Se in the environment is controlled by several biotic and abiotic reduction pathways. Scientists found the SOMs are highly important compounds that can supply carbon to microbe and accelerate the redox reaction of selenium in the environment (Masscheleyn and Patrick 1993; Schulz-Zunkel et al. 2015). Paddy fields undergo a distinct cycle of drying and wetting periods accompanied by redox changes. Iron oxide reductive dissolution results in less sorption to the soil under anoxic conditions compared with oxic conditions (Xu et al. 2011; Fan et al. 2014). However, few studies have reported on the mobilization mechanism of Se during soil Eh change process.

In the present study, the Se release from soil and Fe fractionation change during flooded treatment was investigated. Soil was incubated under flooded (anoxic) conditions to different Eh values with organic matter (OM) addition. Then sequential extraction experiments and X-ray photoelectron spectroscopy (XPS) analysis of incubated soils were carried out to obtain the fractionation and distribution of Se and Fe in soil. In this study, the iron oxide reductive dissolution under different Eh values was evaluated for revealing the transformation mechanism of Se in soil. This information is useful to understand the environmental behaviors of selenite in wetland and paddy soil.

2 Materials and methods

The soil (entisol) used in this study was collected from Shandong Province, China. The soil was air-dried, ground to pass through a 0.85-mm nylon fiber sieve, and stored at room temperature in polyethylene flasks until use. The detailed physiochemical properties of the soil were analyzed and given in Table 1. To simulate soil with a high Se concentration, we added 2 L K_2SeO_3 (analytical grade, Sigma) solution (Se (IV) 625 mg L^{-1}) to 5 kg soil in a polypropylene plastic barrel and mixed the components by gentle swirling. The supernatant was removed after standing for 7 days and then aged for 6 months.

The effects of soil Eh and OM on the Se release dynamics in soil were determined by conducting batch experiments using 50 mL centrifuge tubes (acid-clean) as batch reactors. Four treatments were adopted as follows: (1) low-OM soils, 40 g of original soil was mixed with 20 mL deionized water; (2) high-OM soils, 40 g of original soil and 1.6 g glucose were mixed with 20 mL deionized water; (3) low-OM soils with Se added, 40 g of soil with added Se (aged for 6 months) was mixed with 20 mL of deionized water; (4) high-OM soils with Se added, 40 g of soil with added Se (aged for 6 months) and 1.6 g of glucose were mixed with 20 mL of deionized water. Each treatment included eighteen tubes and all tubes were sealed with a screw cap, and Teflon seal tape was used to close the tube. All samples were incubated in the glove box (99.99% N_2 atmosphere) in dark at 25 °C. At a given reaction time (day 2, 4, 8, 15, 28, or 56), three sample tubes per treatment were randomly collected for Eh, pH, and Se and Fe analyses. On each sampling day, pH and Eh were initially measured using a commercial glass reference electrode (pHS-3B, REX, China) and an oxidation–reduction potentiometer (AZ8551, AZ, China). Afterward, the samples were centrifuged at 9000 rpm and the supernatant was filtered by using 0.22-μm cellulose filters, and soil samples were freezed at −70 °C. In addition, control experiment was conducted to

Table 1 Location and some properties of soils

Location	pH (1:2.5)	OM (%)	Fe_{total} (%)	Al_{total} (%)	Mn_{total} (mg kg^{-1})	Fe_{OX} (mg kg^{-1})	Al_{OX} (mg kg^{-1})	Mn_{OX} (mg kg^{-1})	Fe_{DCB} (mg kg^{-1})	Al_{DCB} (mg kg^{-1})	Mn_{DCB} (mg kg^{-1})	Se (mg kg^{-1})	Texture % (*v*/*v*)		
													Clay (%)	Silt (%)	Sand (%)
Liaocheng	6.7	1.37	2.55	4.63	274	351	294	106	429	74.0	127	0.38	5.00	35.8	59.2

Fe_{OX}, Al_{OX}, Mn_{OX}: amorphous Fe, Al, and Mn extracted by acidified ammonium oxalate buffer
Fe_{DCB}, Al_{DCB}, Mn_{DCB}: dithionite-bicarbonate-citrate (DCB) extractable Fe, Al, and Mn

obtain the data of Se release from soil under air circulation, and detailed experimental design was given in the Electronic Supplementary Material.

Water-soluble and ligand-exchangeable Se were sequentially extracted using Milli-Q water (18.2 MΩ) and 0.1 M $KH_2PO_4 + K_2HPO_4$ buffer (P-buffer, pH 7.0), respectively (Kulp and Pratt 2004). Samples were first weighed (1 g) into a 50-mL centrifuge tube. Milli-Q water (10 mL) was added and the tube was shaken on a reciprocating shaker (175 oscillations min^{-1} at room temperature) for 2 h. After centrifugation (3500 r min^{-1}; 20 min), the supernatant was decanted into a polyethylene vessel. The residue was washed with 10 mL Milli-Q water and the above procedures were repeated. Subsequently, 10 mL of 0.1 M P-buffer (pH 7.0) was added to the residue from the water extraction. The aforementioned procedures were repeated, and then 10 mL of Milli-Q water was added for rinsing. The supernatant water was combined with the previous P-buffer extract. The organic matter associated Se and others extraction followed methods (Kulp and Pratt 2004). The Se and Fe concentrations in the filter liquor were measured by hydride generation atomic fluorescence spectrometry (HG-AFS, AFS-230E, Haiguang, China) and inductively coupled plasma atomic emission spectroscopy (ICP7500, Shimadzu, Japan), respectively.

Soils collected on days 0, 15, and 56 were analyzed by XPS (Escalab 250Xi, Thermo Fisher Scientific, USA). All samples were freeze-dried and ground to fine powder prior to XPS measurement. XPS spectra were obtained using a monochromatized Al Kα X-ray source (1486.6 eV), and the analytical chamber pressure was below 6×10^{-8} Pa. Survey spectra (0–1100 eV) were obtained at a constant analyzer pass energy of 150 eV and step size of 1 eV. High-resolution scans were conducted depending on the examined peak with a pass energy of 30 eV and step size of 0.1 eV. The oxidation status of Fe and Se was acquired by obtaining the narrow scan spectra for Fe $2p_{3/2}$ and Se $3d_{5/2}$. The carbon 1 s electron binding energy corresponding to graphitic carbon at 284.8 eV was adopted as reference for calibration. The narrow scan spectra for Fe $2p_{3/2}$ and Se $3d_{5/2}$ were collected in binding energy forms and analyzed using a nonlinear least-squares curve-fitting program (XPSPEAK41 software).

Meanwhile, transmission electron microscopy (TEM) analysis was conducted for soils collected on days 0 and 56. Freeze-dried soil samples were passed through a 2-mm sieve and dispersed in ethanol under sonication (45 kHz, 10 min). The suspension was dropped onto a copper grid with carbon film (200 mesh). Samples were imaged by TEM (Tecnai-G20, FEI, USA) at an accelerating voltage of 200 kV. The elemental composition of nanoparticles in a specific area was examined by EDS (EDAX, USA) with a super-ultrathin window sapphire detector.

3 Results and discussion

3.1 Soil characteristics

Soil used in this study was classified as entisols on the basis of American soil taxonomy. Soil characteristics are shown in Table 1. Initially, the soil was neutral at pH 6.7, and SOM content was only 1.37%. The total Fe, Al, and Mn contents in soil were 2.55, 4.63, and 274 mg kg^{-1}, respectively. The amorphous Fe and Mn contents extracted by acidified ammonium oxalate buffer (Fe_{OX}) were 351 and 106 mg kg^{-1}, respectively. The dithionite–bicarbonate–citrate-extractable soil Fe and Mn (Fe_{DCB}) contents were 429 and 127 mg kg^{-1}, and Se concentration was 0.38 mg kg^{-1}.

3.2 Soil solution extraction

3.2.1 Change in Eh and pH

The changes in Eh and pH during anoxic incubation for different treatment soils are presented in Fig. 1. The pH decreased immediately after incubation, but a substantial difference was noted between soils with and without added glucose. The pH of low-OM soil varied slightly. By contrast, the pH of high-OM soils declined by 1.7 or 1.8 pH units for the absence or presence of Se, respectively. A series of redox reactions such as those for NO_3^-/NH_4^+, Mn(IV)/Mn(II), Fe(III)/Fe(II), and CH_2O/CO_2 occurred. When Fe(III)(hydr)oxides are reduced, OH^- is produced, and the pH is expected to increase. In this study, pH declined immediately because of the production of CO_2 and H^+ from the degradation of glucose or other OMs, which exceeded base production. pH started to increase after 15 or 28 days for low- or high-OM soil, respectively, because of the depletion of glucose and other organic matters and the OH^- production exceeding H^+ production (Jensen et al. 1998).

Although the Eh went down in all treatments after the start of incubation, the Eh of the high-OM soils decreased more rapidly than that of low-OM soils. However, the Eh decrease in high-OM soils developed slowly after 2 days of incubation. By contrast, the Eh of low-OM soil (without added Se) decreased for 56 days although the downward trend began to decelerate after 8 days of incubation. The Eh curves indicated that OM degradation can lead to decreased soil Eh under flooded conditions.

3.2.2 Se and Fe concentration in liquid supernatant

As Fig. 2 shows, no Se was detected in supernatant for soils (without Se added). The control experiment was conducted to obtain the data of Se release from soil under air circulation, and the result was shown in Fig. Fig. S1 (Electronic Supplementary Material). The result indicated that the concentration of Se in soil solution was significant increased from 1.44 mg L^{-1} (0.25 day) to 1.48 mg L^{-1} (0.5 day) ($p < 0.05$). However, there is no significant change among Se concentration at sampling time after 0.5 day. The amounts of Se released from the high-OM soil (with added Se) were 2.43 and 3.61 mg L^{-1} for 2 and 4 days of incubation, respectively, and then decreased to 1.14 mg L^{-1} at day 8, followed by slight fluctuations. In contrast, increased Se concentrations were recorded for approximately 2 weeks' incubation of soils in the low-OM treatment. Compared to control experimental result, the Se concentration increased initially and then decreased in all anoxic treatments. Parts of soil Se were released into solution during incubation, and Se speciation in soil was altered. The dissolved Se would transform into a stable chemical speciation, such as elemental Se(0) and metal selenides (Se(II)). In organic-rich marshland soils, selenium-containing precipitate as elemental Se(0) and metal selenides can be formed under chemically reducing conditions (Hibbs et al. 2017). Moreover, previous studies suggested that associated Se is released into soil solution, because of the microbial degradation of OM and reductive dissolution of soil minerals (such as iron hydroxides) (Shaheen et al. 2017). Numerous Se transformations can also occur in the presence of microbes. For example, immobilization of Se as Se^0 can occur under oxidative or reductive conditions (Février et al. 2007; Ashworth et al. 2008).

In general, iron oxides or hydroxides in soil are reduced and dissolved under anoxic conditions, with ferrous ions released into the soil solution. In this study, the Fe concentration in each collected sample was determined, and the results are expressed in Fig. 2. Initially, few Fe ions were detected in low-OM soil systems, whereas the Fe concentration increased with incubation time in high-OM soil systems. However, results showed that Fe release was influenced by Se content in high-OM soils. Within 8 days of incubation, the concentration of Fe released from high-OM soil (without added Se) increased sharply and reached 216 mg L^{-1} on day 8. During incubation, in high-OM soil (without added Se) treatment, the Fe concentration released conformed to the first-order dynamic equation (equation 1 in Table 2). By contrast, the Fe concentration released from high-OM soil (with added Se) increased slightly in the 8 days of incubation. Only 7.49 mg L^{-1} Fe was detected on day 8, and the relationship of Fe concentration and time (d) fitted a linear equation (equation 3 in Table 2). However, Fe concentration increased markedly in the later days (from day 8 to 56) and reached 544 mg L^{-1} on day 56. This relation was fitted to the linear equation (equation 3 in Table 2).

The comparison of Se and Fe changes during incubation suggests that the Se released into supernatant reacts with Fe and results in the following three possible scenarios. (1) Se(IV) is reduced by Fe^{2+} to elemental Se or selenides, which exhibits decreased solubility, and Fe^{2+} may transform into

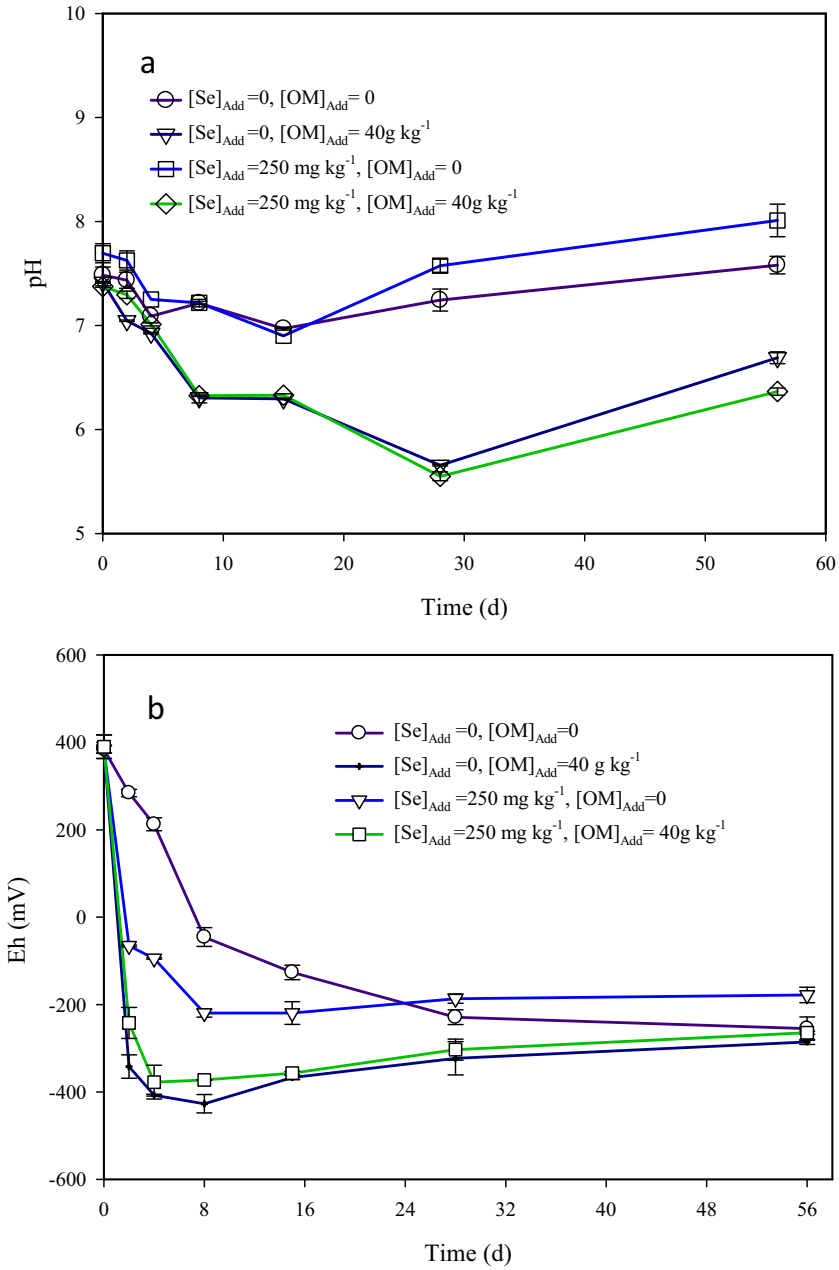

Fig. 1 Changes of pH (**a**) and Eh (**b**) in soil suspension liquid at different incubation times

Fe(III). By contrast, Fe(III) exists as Fe oxide precipitates in our experimental condition, because Fe solubility in soils tends to stabilize near the ion activity product of $(Fe^{3+})(OH^{-})^3 = 10^{-39.3}$ (Norvell and Lindsay 1982a, b). (2) Under anaerobic conditions, the transformation change of iron oxides occurs with reductive dissolution, and the amount of amorphous iron oxides with large special area increases providing additional sorption sites for Se. Fan et al. reported that soils with low Eh exhibit high sorption capacities for As and Sb because of the transformation of soil iron oxides (Fan et al. 2014; Fan et al. 2016). (3) Fe^{2+} reacts with Se, and several insoluble compounds, such as ferrous selenide (FeS), ferrous diselenide ($FeSe_2$), ferric selenite ($Fe_2(OH)_4SeO_3$), or other Fe–Se precipitates, are produced (Scheinost and Charlet 2008; Eswayah et al. 2017). (4) OM in soil can be used by Fe or Se reducing microorganisms as carbon sources and electron donors, and those microorganisms can enhance reduction of Fe and Se in soil (Eswayah et al. 2016; Shaheen et al. 2017).

3.3 Se speciation in the soil

3.3.1 Sequential extraction analysis

Sequential extraction experiments were carried out to determine the changes in Se speciation in differently treated soils with incubation time. The Se concentrations in the low-OM

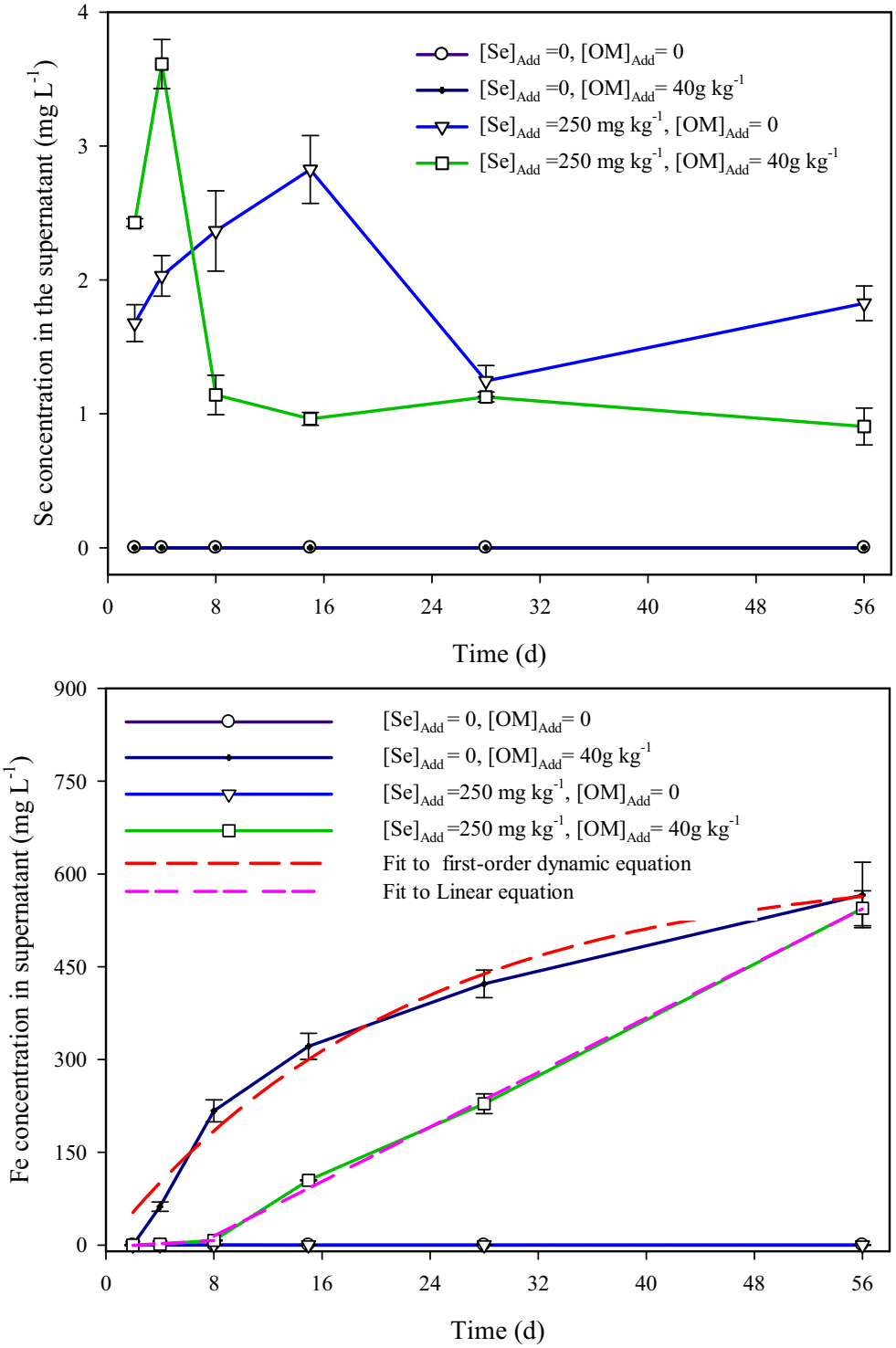

Fig. 2 Concentration of Se and Fe in soil solutions extracted at different times of incubation

soil before incubation were 17.5, 16.3, 40.5, and 161 mg kg^{-1} for water-soluble Se, ligand-exchangeable Se, OM–Se fractions, and other Se fractions (elemental and residual Se contents), respectively (Fig. 3). However, the content of Se existing as different species varied with incubation time. In the low-OM soil system, the Se distribution did not significantly change in the first 2 days of incubation. The water-soluble Se concentration only decreased to 16.5 mg kg^{-1} on day 2 of incubation, and the ligand-exchangeable and OM–Se decreased to 14.3 and 39.5 mg kg^{-1}, respectively. By contrast, the water-soluble Se, ligand-exchangeable Se, and OM–Se concentrations dropped to 4.21, 6.08, and 32.0 mg kg^{-1} on day 15 of incubation for low-OM soil. Relative to those in the high-OM soil, the water-soluble Se concentration declined

Table 2 Regression models for the concentration of Fe (mg L^{-1}) and incubation time (day)

No. of equation	Regression model	Constant result and units		R^2
		a	k	
1	$C_{Fe} = a \times (1\text{-}exp^{kt})$,	613.6 (mg L^{-1})	− 0.0448 (day^{-1})	0.990
2	$C_{Fe} = -2.96 + 1.28 \times t$	− 2.96 (mg L^{-1})	1.28 (mg L^{-1} day^{-1})	0.991
3	$C_{Fe} = -73.5 + 11.0 \times t$,	− 73.5 (mg L^{-1})	11.0 (mg L^{-1} day^{-1})	0.999

from 15.2 mg L^{-1} (incubation day 0) to 5.88 mg L^{-1} (incubation day 2) and 0.213 mg kg^{-1} (incubation day 15), respectively. Meanwhile, the elemental and residual Se concentration in high-OM soil increased to 204 from 176 mg kg^{-1} within 15 days of incubation. Results dedicated that Se bioavailability was expected to decrease with anaerobic incubation time, because the selenium extracted using water and P-buffer represents the major Se forms available for plant uptake (Sharmasarkar and Vance 1995; Kulp and Pratt 2004). Moreover, the addition of glucose accelerated the transformation of Se because glucose provides a carbon source to microbes. Several studies demonstrated that microbes can enhance the reduction of toxic Se oxyanions (SeO_4^{2-} and SeO_3^{2-}) to the insoluble and less bioavailable elemental selenium (Se^0) (Eswayah et al. 2016; Eswayah et al. 2017).

3.3.2 XPS analysis

XPS is typically used for analyzing elemental compositional and chemical states on surfaces, especially metalloid transformation on mineral surfaces (Abdel-Samad and Watson 1997; Xu et al. 2011). In this study, XPS was used to determine the speciation of Se and Fe in soil. Figure 4a shows the Se 3*d* XPS spectroscopic data of soils with added Se under different incubation times and OM contents. As reported, the binding energy of the Se 3*d* peak centered at 59.1 eV for Se(IV), 61.6 eV for Se(VI), 54.6–57.5 eV for elemental Se, and 52.8–55.7 eV for metallic selenide compounds (http://srdata.nist.gov/xps; Shenasa et al. 1986; Hamdadou et al. 2002; Naveau et al. 2007; Han et al. 2013). The main peaks were found in the range of 56.0–57.5 eV, as indicated by the elemental Se signal peak. The binding energy of the main peak shifted to lower values, and the peak shape varied with incubation time. When the high-OM soil was incubated for 56 days, two shoulder peaks appeared in the range of 54.0–55.7 eV, which corresponded to signals for metallic selenide compounds. Unlike that in the high-OM soil system, this phenomenon did not occur significantly in the low-OM soil system. In addition, the peak for Se(IV) at 59.1 eV became less evident with prolonged incubation time. In addition, the Se $3d_{5/2}$ peaks of Se(IV), elemental Se, and selenides compounds were selected at 59.1, 57.0, and 55.2 eV, respectively. The parameters were used in fitting high-spin Se compounds with small deviations and the peaks followed the Gupta and Sen (GS) predictions well, and results were shown in Fig 4b–d and Table 3. Therefore, three results were obtained from Se 3*d* XPS data. First, elemental Se was the main form of Se in the studied soils and indicated that

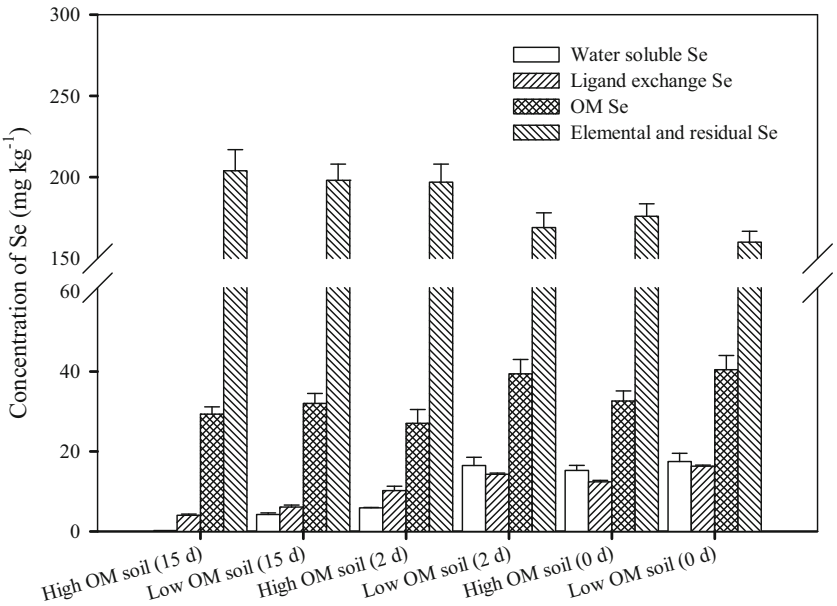

Fig. 3 Se fractions in soils at different times of incubation

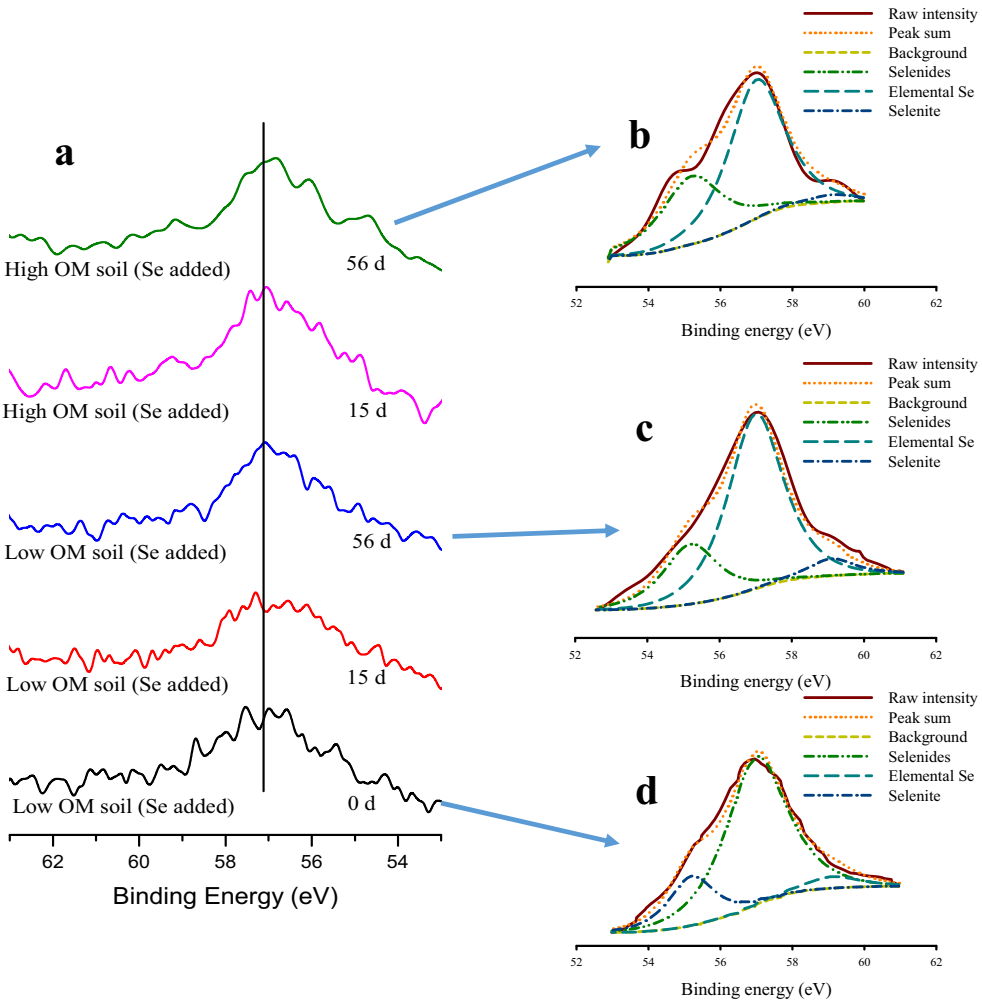

Fig. 4 **a**: Se 3*d* XPS spectra of low- and high-OM soils at different incubation times; **b**: Se $2d_{5/2}$ XPS spectra of low-OM soils with Se added at 0 day of incubation; **c**: Se $2d_{5/2}$ XPS spectra of low-OM soils with Se added at 56 days of incubation; **d**: Se $2d_{5/2}$ XPS spectra of high-OM soils with Se added at 56 days of incubation

Se(IV) was reduced to Se^0 in the soil within the 6 months of sorption and aging procedures, because there are about three quarter of Se determined as Se^0. Second, soil Se(IV) sorption can be reduced to a lower-state Se, such as Se^0 and Se(II), during the anaerobic incubation process. Third, the formation of metallic selenides was enabled in soil under anaerobic conditions, especially in high-OM soil.

Several studies reported the biogeochemical cycle of Se in wetland soil Se(IV) was reduced to Se(0) under wetland conditions (Yamada et al. 1999), and Se(0) formation and metallic selenides at low Eh can limit Se solubility (Masscheleyn and Patrick 1993). Meanwhile, Se formation can be affected by OMs in a wetland system. For example, the major Se form in paddy soil was organic sulfide matter-bound Se and Se(0), which accounted for more than 50% of the total Se (Zhang and Moore 1996). Moreover, Fe and Mn oxide-bound Se was the dominant fraction in the non-flooded soil (Wang et al. 2012), and the sorption capacity of Se on Fe and Mn oxides was diminished under flooded conditions because of the reduction of Fe and Mn oxides (Wan et al. 2013). Thus, OM content and Fe oxide formation can influence the Se transformation and bioavailability in soil.

Table 3 Binding energies (BE), full width at half maximum (FWHM), and area percentage for peaks in the Se $3d_{5/2}$ XPS spectra of soil for various incubation times

Peak	BE (eV)	Low-OM soil(with Se added) 0 day		Low-OM soil (with Se added) 56 days		High-OM soil (with Se added) 56 days	
		Area (%)	FWHM (eV)	Area (%)	FWHM (eV)	Area (%)	FWHM (eV)
1	55.2	19.02	2.0	24.08	1.8	34.18	2.0
2	57.0	75.68	1.8	70.21	1.8	62.81	1.8
3	59.1	5.30	1.5	5.71	1.5	3.01	1.6

3.4 Soil Fe analysis

The Fe 2*p* of the soil on days 0, 15, and 56 was collected (Fig. 5). Results expressed that the Fe 2*p* peak positions of the soil varied with different treatments. However, the incubation time did not markedly influence the peak position of the low-OM soil (without added Se). In contrast, the peak position of high-OM soils (with added Se) shifted to lower binding energies with incubation time, and the peak shape varied with different treatments. According to previous studies, the XPS peak depends on the oxidation states of Fe and the crystallinity degree (Roosendaal et al. 1999; Ruby et al. 2000; Yamashita and Hayes 2008). Therefore, certain changes occurred in the formation of iron oxides in soil subjected to anoxic conditions.

The formation change of Fe in the soil with incubation time and OM content was investigated by selecting the Fe $2p_{3/2}$ peak, analyzing iron oxide formation in soil, and determining the influence of incubation conditions on the iron oxide speciation. Such investigations were conducted because of the stronger and narrower Fe $2p_{3/2}$ peak compared with the Fe $2p_{1/2}$ peak. Various Fe compounds, including FeS_2, FeO, Fe_3O_4, Fe_2O_3, and FeOOH, exist in soil. On the basis of previous studies, the Fe $2p_{3/2}$ main peak positions of FeS_2, FeO, Fe_3O_4, Fe_2O_3, and FeOOH were 706.7, 708.3, 709.8, 710.6, and 711.6 eV, respectively (Grosvenor et al. 2004; Scott et al. 2005; Yamashita and Hayes 2008). Meanwhile, three peaks at 713.1, 714.5, and 716.0 eV were considered as the surface peak. The parameters were used in fitting high-spin Fe compounds with small deviations, and the peaks followed the Gupta and Sen (GS) predictions well. Figure 6 shows the Fe $2p_{3/2}$ XPS spectra from soils under different treatments, and the fitting results are given in Table 4. Results indicate that the proportion of Fe(II) compounds increased with incubation time in low-OM soil without added Se and that the surface peaks at 713.1 and 714.5 eV changed after incubation. This result means that the relative intensity of the surface structure changed during incubation. Moreover, glucose addition enhanced the increase in Fe(II) compounds, given the proportion of peaks at 708.3 eV were 3.9 and 7.2% in low-OM and high-OM soils, respectively, of 15 days of incubation. Furthermore, considerable differences were observed between the low-OM soil samples with and without added Se before incubation; moreover, the proportions of surface peaks at 713.1 and 714.5 eV in the low-OM soil with added Se were larger than those of the low-OM soil only because Se sorption experiments persisted for 1 week and reductive dissolution of Fe oxides occurred in this process. The results suggest that multiple causes are explaining the presence of surface peaks with increased binding energy. A possible cause of the surface structure is the reduced coordination of surface molecules. With decreased coordination, the Fe^{3+} ion becomes surrounded by a diminished electron density, which requires additional energy to produce a photoelectron (Yamashita and Hayes 2008). Thus, the crystalline state of the iron oxides in the soil altered after anoxic treatments, and some amorphous phase iron oxides were formed. Meanwhile, a change in surface microtopography of soil after incubation (Fig. 7) was observed using high-resolution TEM (HR-TEM). This finding indicates the formation of poorly crystalline particles after incubation especially in the high-OM soil.

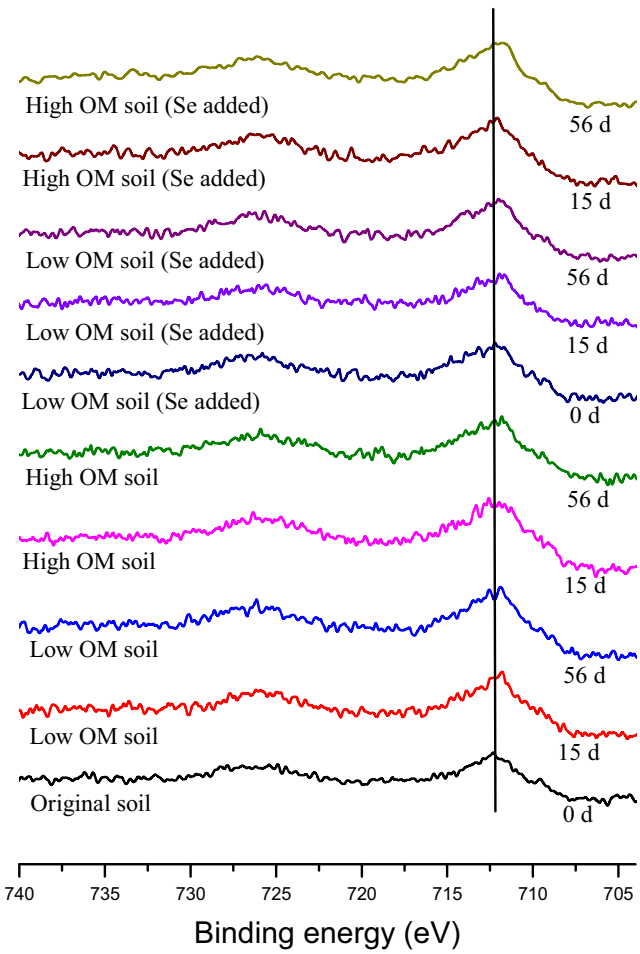

Fig. 5 Fe 2*p* XPS spectra of soils at different incubation times

3.5 Mechanism of Se reduction in soil

Under anoxic conditions, Se concentration in supernatants and Se formation in soils varied with incubation time and soil OM content. However, the XPS and extraction results show that the main proportion of Se existed as Se(0) in soil, and metallic selenides were produced during incubation. Glucose addition also enhanced Se and Fe reduction. Thus, the possible routes of Se transformation mechanisms in soil are suggested as follows: (i) Se(IV) is sorbed onto the soils initially when exogenous selenium enters into soil, and Se(IV) is reduced to less

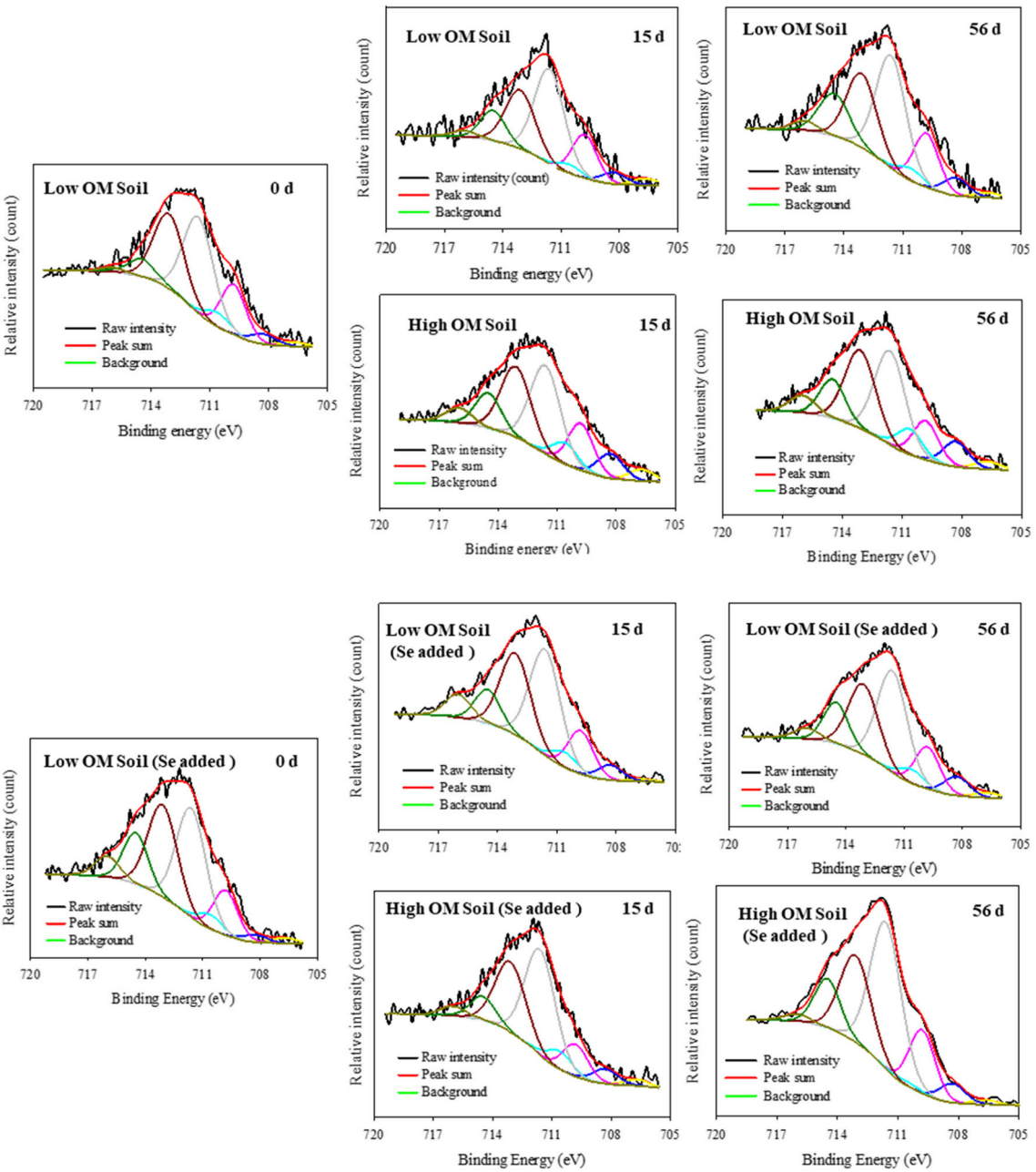

Fig. 6 Fe $2p_{3/2}$ XPS spectra of soils of different treatments at 0, 15, 56 days of incubation

soluble forms by soil minerals or OM. Some studies demonstrated that Se can be reduced in the presence of organic agents and humic acid (Struyk and Sposito 2001; Yang et al. 2016). (ii) Se(IV) is reduced by dissolved Fe^{2+} in solution, and Se(0) is produced during incubation. (iii) Fe^{2+} reacts with Se^{2-}, and FeSe forms, which is controlled by iron hydroxide dissolution. (iv) The effect of dissimilatory Se reduction on environmental Se pollution remediation mainly involves the transformation of Se into less soluble forms, thus attracting research attention. Previous studies have shown that certain bacteria use Se(VI) as a terminal electron acceptor for anaerobic respiration and utilize OMs as electron donors (Nancharaiah and Lens 2015). Therefore, microorganisms and OAs may play a key role in the Se reduction process.

4 Conclusions

Soils were incubated for more than 56 days, and soil pH and Eh varied with different treatments. High OM content led to substantial changes in soil solution characteristics, including pH, Eh, and Se and Fe concentrations. Se concentration

Table 4 Binding energies (BE), full width at half maximum (FWHM), and area percentage for peaks in the Fe $2p_{3/2}$ XPS spectra of soil for various incubation times

Peak	BE (eV)	FWHM (eV)	Area (%)									
			Low-OM soil			High-OM soil		Low-OM soil (with Se added)			High-OM soil (with Se added)	
			0 day	15 days	56 days	15 days	56 days	0 day	15 days	56 days	15 days	56 days
1	706.7	1.5	1.62	2.12	2.38	3.34	2.17	1.43	1.88	1.58	0.67	1.01
2	708.3	1.5	3.35	3.9	4.75	7.2	7.03	1.87	4.66	5.67	4.18	4.36
3	709.8	1.5	16.2	15	14.5	13.6	10.8	11.6	10.2	12.3	12	14.8
4	710.6	1.5	4.63	3.01	3.26	6.23	7.07	3.64	5.77	4.15	4.18	1.01
5	711.6	1.8	37.2	39.2	36.1	30.7	31.3	34	40.2	36	35.6	41.2
6	713.1	1.8	29	24.2	23.8	24.5	26.1	28.7	26.9	24.9	27.4	24.5
7	714.5	1.5	6.56	10.4	12.7	10.1	10.8	13.3	7.43	12.1	9.44	11.5
8	716.0	1.5	1.44	2.17	2.51	4.33	4.73	5.46	2.96	3.21	6.53	1.62

increased initially and then decreased for all treatments. In the high-OM soil without added Se, the Fe concentration in soil solution conformed to first-order dynamic equation during incubation time, and the Fe concentration reached 216 mg L^{-1} on day 8. By contrast, Fe concentration released from high-OM soil (with added Se) increased slightly within 8 days of incubation. In particular, only 7.49 mg L^{-1} Fe was detected on day 8, and a growth spurt occurred. Extraction analyses also revealed that parts of Se in soil can be released into solution during incubation, and the speciation of Se in the solution changed. Relative to that in low-OM soil, the water-soluble Se content in the high-OM soil decreased to 5.88 and 0.213 mg kg^{-1} on incubation days 2 and 15, respectively. XPS revealed that the primary speciation of Se in soil was elemental Se, and metallic selenides were increased with aerobic incubation prolonged. Moreover, the fractions of soluble and exchanged Se decreased with incubation time. Furthermore, XPS and HR-TEM data presented that the crystalline state of

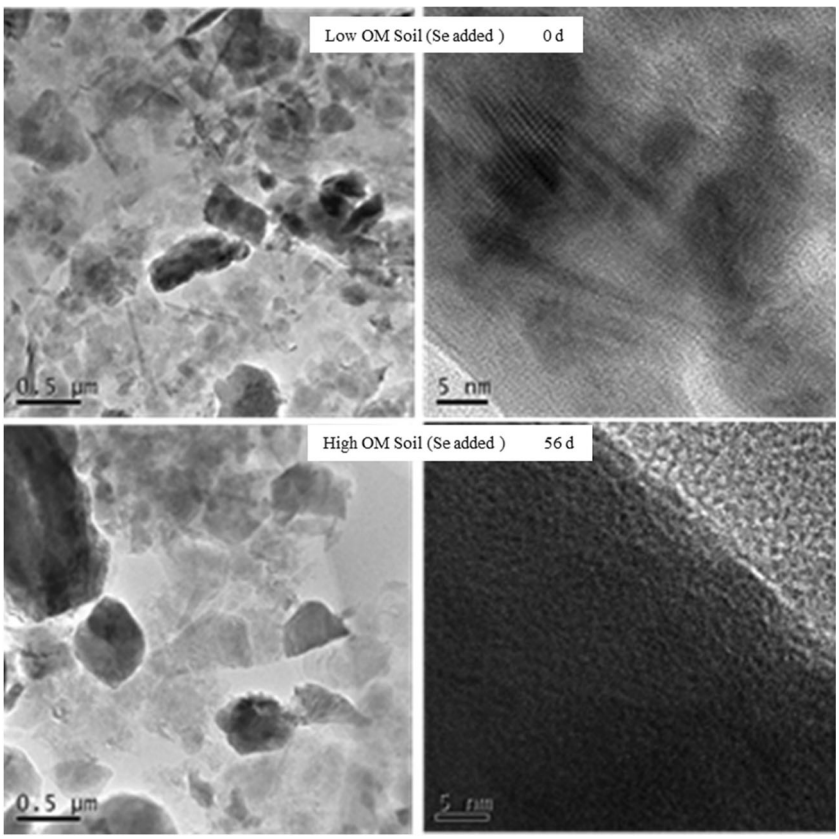

Fig. 7 TEM micrographs of soils of low-OM soil (0 day of incubation) and high-OM soil (56 days of incubation)

iron oxides in soil altered after anoxic treatments, and amorphous phase iron oxides were formed. This study can help explain the environmental behavior of high Se concentrations entering soils, especially wetting soils or paddy soil.

Funding information This work was financially supported by the National Natural Science Foundation of China (No. 41401255, 51508057), the Natural Science Foundation of Chongqing of China (No. cstc2015jcyjA20018), China Postdoctoral Science Foundation (2016M602633), Chongqing Postdoctoral Science Foundation Special Funded Project (Xm2017048), and Innovation Project of University Students' Research in Chongqing (201710618024).

References

Abdel-Samad H, Watson PR (1997) An XPS study of the adsorption of chromate on goethite (α-FeOOH). Appl Surf Sci 108:371–377

Ashworth DJ, Moore J, Shaw G (2008) Effects of soil type, moisture content, redox potential and methyl bromide fumigation on Kd values of radio-selenium in soil. J Environ Radioact 99:1136–1142

Chakraborty S, Bardelli F, Charlet L (2010) Reactivities of Fe(II) on calcite: selenium reduction. Environ Sci Technol 44:1288–1294

Combs GF (2007) Selenium in global food systems. Brit J Nutr 85:517–547

Dhillon KS, Dhillon SK (1999) Adsorption-desorption reactions of selenium in some soils of India. Geoderma 93:19–31

Eswayah AS, Smith TJ, Gardiner PHE (2016) Microbial transformations of selenium species of relevance to bioremediation. Appl Environ Microbiol 82:4848–4859

Eswayah AS, Smith TJ, Scheinost AC, Hondow N, Gardiner PHE (2017) Microbial transformations of selenite by methane-oxidizing bacteria. Appl Microbiol Biotechnol 101:6713–6724

Fan JX, Wang YJ, Liu C, Wang LH, Yang K, Zhou DM, Li W, Sparks DL (2014) Effect of iron oxide reductive dissolution on the transformation and immobilization of arsenic in soils: new insights from X-ray photoelectron and X-ray absorption spectroscopy. J Hazard Mater 279:212–219

Fan J-X, Wang Y-J, Fan T-T, Dang F, Zhou D-M (2016) Effect of aqueous Fe(II) on Sb(V) sorption on soil and goethite. Chemosphere 147:44–51

Février L, Martin-Garin A, Leclerc E (2007) Variation of the distribution coefficient (Kd) of selenium in soils under various microbial states. J Environ Radioact 97:189–205

Grosvenor AP, Kobe BA, Biesinger MC, McIntyre NS (2004) Investigation of multiplet splitting of Fe 2p XPS spectra and bonding in iron compounds. Surf Interface Anal 36:1564–1574

Hamdadou N, Bernède JC, Khelil A (2002) Preparation of iron selenide films by selenization technique. J Cryst Growth 241:313–319

Han DS, Batchelor B, Abdel-Wahab A (2013) XPS analysis of sorption of selenium(IV) and selenium(VI) to mackinawite (FeS). Environ Prog Sustain 32:84–93

Hibbs BJ, Lee M, Ridgway R (2017) Land use modification and changing redox conditions releases selenium and sulfur from historic marsh sediments. J Contemp Water Res Edu 161:48–65

Hingston FJ, Posner AM, Quirk JP (1968) Adsorption of selenite by goethite, adsorption from aqueous solution. Am Chem Soc:82–90

Jensen MB, Hansen HCB, Nielsen NE, Magid J (1998) Phosphate mobilization and immobilization in two soils incubated under simulated reducing conditions. Acta Agric Scand Sect B Soil Plant Sci 48:11–17

Kulp TR, Pratt LM (2004) Speciation and weathering of selenium in upper cretaceous chalk and shale from South Dakota and Wyoming, USA. Geochim Cosmochim Acta 68:3687–3701

Lessa JHL, Araujo AM, Silva GNT, Guilherme LRG, Lopes G (2016) Adsorption-desorption reactions of selenium (VI) in tropical cultivated and uncultivated soils under Cerrado biome. Chemosphere 164:271–277

Manceau A, Charlet L (1994) The mechanism of selenate adsorption on goethite and hydrous ferric oxide. J Colloid Interf Sci 168:87–93

Masscheleyn PH, Patrick WH (1993) Biogeochemical processes affecting selenium cycling in wetlands. Environ Toxicol Chem 12:2235–2243

Medicine, F.a.N.B.-U.I.o (2000) Dietary references intakes for vitamin C, vitamin E, selenium and carotenoids. National Academy Press, Washington

Myneni SCB, Tokunaga TK, Brown GE (1997) Abiotic selenium redox transformations in the presence of Fe(II,III) oxides. Science 278:1106–1109

Nancharaiah YV, Lens PNL (2015) Ecology and biotechnology of selenium-respiring bacteria. Microbiol Mol Biol Rev 79:61–80

Naveau A, Monteil-Rivera F, Guillon E, Dumonceau J (2007) Interactions of aqueous aelenium (−II) and (IV) with metallic sulfide surfaces. Environ Sci Technol 41:5376–5382

NIST X-ray photoelectron spectroscopy database, NIST standard reference database 20, version https://srdata.nist.gov/xps/Default.aspx

Norvell WA, Lindsay WL (1982a) Effect of ferric-chloride additions on the solubility of ferric ion in a near-neutral soil. J Plant Nutr 5:1285–1295

Norvell WA, Lindsay WL (1982b) Estimation of the concentration of estimation of the concentration of Fe^{3+} and the $(Fe^{3+})(OH^{-})_3$ ion product from equilibria EDTA in soil. Soil Sci Soc Am J 46:710–715

Rayman MP (2008) Food-chain selenium and human health: emphasis on intake. Br J Nutr 100:254–268

Roosendaal SJ, van Asselen B, Elsenaar JW, Vredenberg AM, Habraken FHPM (1999) The oxidation state of Fe(100) after initial oxidation in O_2. Surf Sci 442:329–337

Rotruck JT, Pope AL, Ganther HE, Swanson AB, Hafeman DG, Hoekstra WG (1973) Selenium: biochemical role as a component of glutathione peroxidase. Science 179:588–590

Ruby C, Humbert B, Fusy J (2000) Surface and interface properties of epitaxial iron oxide thin films deposited on MgO(001) studied by XPS and Raman spectroscopy. Surf Interface Anal 29:377–380

Sathe SK, Mason AC, Rodibaugh R, Weaver CM (1992) Chemical form of selenium in soybean (Glycine max L.) lectin. J Agric Food Chem 40:2084–2091

Scheinost AC, Charlet L (2008) Selenite reduction by mackinawite, magnetite and siderite: XAS characterization of nanosized redox products. Environ Sci Technol 42:1984–1989

Schulz-Zunkel C, Rinklebe J, Bork H-R (2015) Trace element release patterns from three floodplain soils under simulated oxidized–reduced cycles. Ecol Eng 83:485–495

Scott TB, Allen GC, Heard PJ, Randell MG (2005) Reduction of U(VI) to U(IV) on the surface of magnetite. Geochim Cosmochim Acta 69:5639–5646

Shaheen SM, Frohne T, White JR, DeLaune RD, Rinklebe J (2017) Redox-induced mobilization of copper, selenium, and zinc in deltaic soils originating from Mississippi (USA) and Nile (Egypt) River Deltas: a better understanding of biogeochemical processes for safe environmental management. J Environ Manag 186:131–140

Sharmasarkar S, Vance GF (1995) Fractional partitioning for assessing solid-phase speciation and geochemical transformations of soil selenium. Soil Sci 160:43–55

Shen DZ, Fan JX, Zhou WZ, Gao BY, Yue QY, Kang Q (2009) Adsorption kinetics and isotherm of anionic dyes onto organo-

bentonite from single and multisolute systems. J Hazard Mater 172(1):99–107

Shenasa M, Sainkar S, Lichtman D (1986) XPS study of some selected selenium compounds. J Electron Spectrosc Relat Phenom 40:329–337

Struyk Z, Sposito G (2001) Redox properties of standard humic acids. Geoderma 102:329–346

Tan JA, Zhu W, Wang W, Li R, Hou S, Wang D, Yang L (2002) Selenium in soil and endemic diseases in China. Sci Total Environ 284:227–235

Wan XM, Tandy S, Hockmann K, Schulin R (2013) Changes in Sb speciation with waterlogging of shooting range soils and impacts on plant uptake. Environ Pollut 172:53–60

Wang SS, Liang DL, Wang D, Wei W, Fu DD, Lin ZQ (2012) Selenium fractionation and speciation in agriculture soils and accumulation in corn (Zea mays L.) under field conditions in Shaanxi Province, China. Sci Total Environ 427:159–164

Winkel L, Vriens B, Jones G, Schneider L, Pilon-Smits E, Bañuelos G (2015) Selenium cycling across soil-plant-atmosphere interfaces: a critical review. Nutrients 7:4199–41239

Xu W, Wang H, Liu R, Zhao X, Qu J (2011) Arsenic release from arsenic-bearing Fe–Mn binary oxide: effects of Eh condition. Chemosphere 83:1020–1027

Yamada H, Kase Y, Usuki M, Kajiyama S, Yonebayashi K (1999) Selective determination and formation of elemental selenium in soils. Soil Sci Plant Nutr 45:403–408

Yamashita T, Hayes P (2008) Analysis of XPS spectra of Fe^{2+} and Fe^{3+} ions in oxide materials. Appl Surf Sci 254:2441–2449

Yang Z, Du M, Jiang J (2016) Reducing capacities and redox potentials of humic substances extracted from sewage sludge. Chemosphere 144: 902–908

Zhang YQ, Moore JN (1996) Selenium fractionation and speciation in a wetland system. Environ Sci Technol 30:2613–2619

Zhang P, Sparks DL (1990) Kinetics of selenate and selenite adsorption/desorption at the goethite/water interface. Environ Sci Technol 24: 1848–1856